УДК 539.122

STUDY OF THE PHOTON-STRUCTURE FUNCTION F_2^γ IN THE REACTION $e^+e^- \to e^+e^-$ + hadrons AT LEP2

I. Tyapkin, N. Zimin

The photon-structure function F_2^γ has been studied in the Q^2 range from 10 to 1000 $(\mathrm{GeV/c^2})^2$. The data corresponds to the integrated luminosity of about 220 pb^{-1}, collected by the DELPHI detector during the 1996–1998 LEP runs. Experimental distributions with particular attention on event shape are compared with predictions of the model. The three-component description of DIS proposed in our previous papers is applied here again. A result for Q^2 evolution of the photon-structure function has been obtained.

The investigation has been performed at the Laboratory of High Energies, JINR.

Исследование структурной функции фотона F_2^γ в реакции $e^+e^- \to e^+e^-$ + адроны на LEP2

И. Тяпкин, Н. Зимин

Структурная функция фотона F_2^γ исследовалась в диапазоне Q^2 от 10 до 1000 $(\mathrm{ГэВ/c^2})^2$. Данные соответствуют интегральной светимости около 220 $\mathrm{пб}^{-1}$, полученной на установке DELPHI в сеансах 1996–1998 годов. Распределения экспериментально полученных переменных сравниваются с предсказаниями модели. Особое внимание уделено переменным, описывающим кинематику конечного адронного состояния. Трехкомпонентное описание DIS, предложенное в наших предыдущих работах, применено и в этой работе. Получена Q^2-зависимость структурной функции фотона.

Работа выполнена в Лаборатории высоких энергий ОИЯИ.

1. INTRODUCTION

The photon structure function has been measured in the reaction $e^+e^- \to e^+e^-\gamma\gamma^* \to e^+e^-X$, where X is a multihadronic system and one of the scattered leptons is observed at a large scattering angle (tagging condition) while the other, remaining at a small angle, is undetected (antitagging condition). Here γ is almost a real photon which is probed by the virtual one γ^*. This re-

action can be described as a deep inelastic $e\gamma$ scattering (DIS). The corresponding cross section can be expressed in terms of the photon structure functions $F_2^\gamma(x,Q^2)$ and $F_L(x,Q^2)$:

$$\frac{d\sigma}{dE_{\text{tag}}\, d\cos(\theta_{\text{tag}})} = \frac{4\pi\alpha^2 E_{\text{tag}}}{Q^4 y}[(1+(1-y)^2)F_2^\gamma(x,Q^2) - y^2 F_L(x,Q^2)] \qquad (1)$$

Here $Q^2 = 4E_{\text{tag}}E_{\text{beam}}\sin^2\frac{\theta_{\text{tag}}}{2}$, $x = \frac{Q^2}{Q^2+W^2}$, $y = 1 - \frac{E_{\text{tag}}}{E_{\text{beam}}}\cos^2\theta_{\text{tag}}$, where E_{tag} and θ_{tag} are the energy and polar angle of the tagged lepton and W is the invariant mass of the hadronic system. Due to small values of y in the experimentally accessible region, an influence of the F_L on the cross section is small (about few per cent) and may be neglected in comparison with the statistical uncertainty of these measurements. The photon structure function can be calculated in the perturbative quantum chromodynamics (QCD). Few types of physical processes contribute to the total cross section: a point-like coupling of the photons to a quark-antiquark pair (QPM), the vector meson contribution (VDM) and the resolved photon contribution [I], (RPC). In the present paper the attempt was made to extend a proposed three-component description of DIS in a wider Q^2 region.

2. EVENT SELECTION

A detailed description of the DELPHI detector can be found in [2]. Data used in this analysis were collected with the DELPHI detector at the LEP2 e^+e^- collider during 1996–1998 for the range of centre-of-mass energies from 163 to 188 GeV. The tagged particle was detected by the DELPHI luminometer STIC which covers angular region from 2.4° to 9.7° and forward electromagnetic calorimeter FEMC which covers angles from 10° to 35°. The following criteria were used to select two-photon events with tagging:

1. The energy deposited by the tagged electron (or positron) in the detector must be greater than $0.45 \times E_{\text{beam}}$ (tagging requirement);

2. No additional clusters with energy exceeding $0.3 \times E_{\text{beam}}$ must be observed anywhere in the forward calorimeters (antitagging requirement);

3. The track multiplicity is 3 or more;

4. The total energy of tracks must be greater than 3 GeV;

5. The visible invariant mass of the hadronic system must be greater than 2.5 GeV/c^2;

6. The vector sum of transverse momenta of all particles normalized to E_{beam} must be less than 0.12;

7. The angle between transverse components of the momentum of the tagged particle and that of the hadronic system must be greater than 120° ;

In this analysis we use all the DELPHI calorimeters for the event reconstruction.

The main source of background for the STIC sample was $\gamma\gamma \to \tau\tau$ interactions and their contribution was estimated from a simulaiton as 2.8 pb. Contamination from $\gamma\gamma \to e^+e^-$ was estimated as 1.5 pb. The new sourse of background has been found in this study. Criteria 1 was reduced

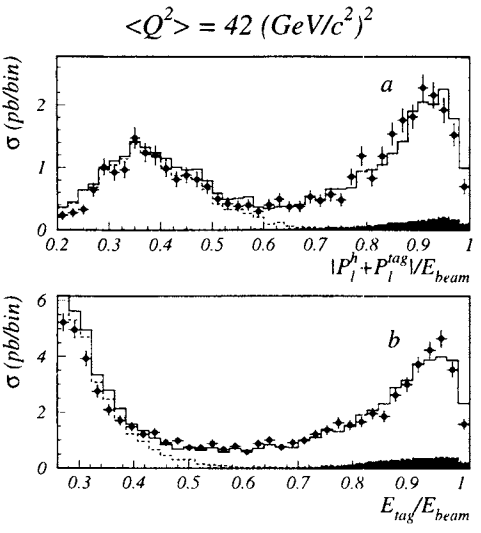

Fig. 1. Distributions for the data compared to the Monte Carlo predictions. a: Longitudinal balance of the event. b: Tagging particle energy normalized to the beam energy. Points are data, and the histograms show the Monte Carlo predictions. QPM+GVDM+RPC — solid line, QPM+GVDM+RPC (with scattered lepton below STIC acceptance) — dashed line, hatched area is the background estimate

down to 0.2 and the $E_{\text{tag}}/E_{\text{beam}}$ distribution together with distribution describing longitudinal balance compered to model prediction in Fig.1. Strong raise in the region of low tagging energies observed in data was well fitted by our model. A special study was made on the level of generated events showing that the most of events in this region are the events with a tagging particle which is well below the STIC acceptance, while high energy particles from the hadronic final state in the low angular region mimic the tagging particle. The majority of those events come from RPC. Thus it is a background to the tagged events. That background can be suppressed by applying the cut on the longitudinal balance in the event (Fig.1b), used in all previous studies, but even in this case a certain fraction of such background will remain in the sample. The background described here is indeed a real limitation on the choice of minimal tagging energy but not an off-momentum or beam-gas background. Finaly, after applying all the criteria, this background was estimated as a 0.8 pb. A contamination from other sources of background was found to be much lower. After background subtraction, the visible cross section of the investigated process was estimated as being 45.3 pb for the sample of events from the 1997–1998 year runs. The average Q^2 for the selected events is about 42 $(\text{GeV/c}^2)^2$.

For the FEMC sample the events from the 1996–1998 year runs were processed together. The background from the $\gamma\gamma \to \tau\tau$ interactions was estimated from a simulation as 0.08 pb. The contamination from other sources of background was found to be much lower. The average Q^2 for the selected events is about 400 $(\text{GeV/c}^2)^2$. After background subtraction the visible cross section for the FEMC sample was estimated as being 1.0 pb. The trigger efficiency was found to be of the order of 98 ± 1% for the selected events.

3. MODELS

A two-photon event generator TWOGAM [3], which was successfully tested in previous DELPHI studies, is based on the exact decomposition of the matrix element of the process. The total cross section is described by the sum of three parts: point-like (QPM), resolved photon con-

tribution (RPC) and soft hadronic (VDM). The QPM and VDM models can be used at any Q^2 and RPC model tested in the region of low Q^2 ($Q^2 < 2$ (GeV / c^2)^2. The RPC can be partially extended in the high Q^2 region by their $\gamma q(g)$ component. For the single or double resolved perturbative part the lowest order diagrams are used. Only the transverse-transverse part of the luminosity function is used in this case. There is no initial or final state parton showering. Strings are formed following the colour flow of the subprocesses and are fragmented according to the LUND model by JETSET [4]. The Gordoiv–Storrow parton density function [5] set 2 was used in this study to produce a sample of events. The kinematics of the partonic system is exact for any photon virtuality. This allows for a smooth suppression of the parton densities of resolved photons when their virtuality increases, according to a more or less theoretically motivated ansatz.

TWOGAM treats exactly the kinematics of the scattered electron and positron, and uses exact (unfactorized) expressions for the two-photon luminosity function. The other available generators are not reproducing the data and so they cannot be used for the cross-check of the results presented here.

4. COMPARISON OF EXPERIMENTAL AND SIMULATED DATA

The success of structure function studies strongly depends on the accuracy of the data description by the model used. This includes the Q^2 and P^2 model dependence, the description of fragmentation and hadronization. Practically that means a good agreement between all the observables in the wider possible region. For example, the RPC component populates relatively more the low E_{tag} region. So, if one restricts his study by the region of high E_{tag} some effects will be less presented and the extracted F_2^γ can be biased. Another example can be the soft hadronic final states. There is a number of limitations from the detectors which do not allow one to study hadronic final states with invariant mass below 3 GeV. This domain is enriched by VDM-like events and not well known. Strongly speaking systematic error in any photon structure function study cannot be treated too seriously before one will study the region of low E_{tag} and W. These examples are only few from the list. In such a situation it is extremely important to use a number of models and generators well describing data for the estimation of systematic error. Unfortunately at the moment we have only TWOGAM which describes data reasonably well.

It was mentioned in our previous study that the model prediction for the RPC component tends to have too high cross section of the high Q^2. Now this observation has been confirmed due to high statistics collected in the region of $Q^2 > 50$ (GeV/c^2)^2. The fit of Q^2 dependence for the RPC component to the data was done and scale dependent suppression function for the RPC component has been evaluated from this fit. The suppression factor runs from 1 to 0 with Q^2 running from the p_t of initial quark system to $10p_t$. This suppressed RPC has been used for all the comparisons below. A lot of observables have been compared to the TWOGAM predictions and all of them are found to be in reasonable agreement. In Fig.2, the event variables involved directly in the structure function measurements are shown. In Fig.3, the same variables are compared to

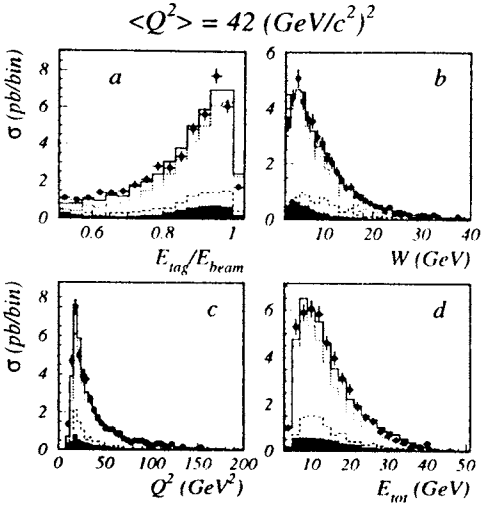

Fig. 2. Distributions for the data compared to the Monte Carlo predictions. a: Energy of tagged particle normalized to the beam energy, b: invariant mass, c: Q^2, d: Total energy of hadronic system. Points are data, and the histograms show the Monte Carlo predictions. QPM+GVDM+RPC — solid line, GVDM+QPM — dotted line, GVDM — dashed line, hatched area is the background estimate

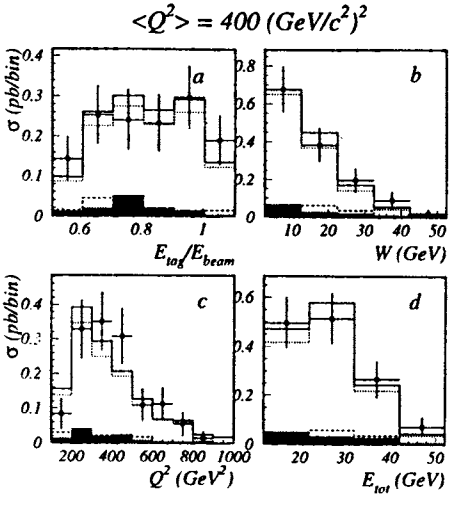

Fig. 3. Distributions for the data compared to the Monte Carlo predictions. a: Energy of tagged particle normalized to the beam energy, b: invariant mass, c: Q^2 , d: Total energy of hadronic system. Points are data, and the histograms show the Monte Carlo predictions. QPM+GVDM+RPC — solid line, GVDM+QPM — dotted line, GVDM — dashed line, hatched area is the background estimate

Fig. 4. Comparison between data and Monte Carlo predictions. Hadronic energy flow in the jets as a function of pseudorapidity for different Q^2. Points are data, and the histograms show the Monte Carlo predictions. QPM+GVDM+RPC — solid line, GVDM+QPM — dashed line, GVDM — dotted line

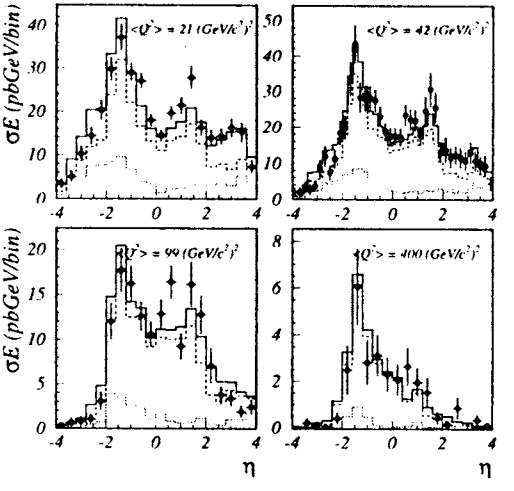

the model prediction for the sample with tagging from forward electromagnetic calorimeter (FEMC).

The statistics collected makes possible the division of ST1C sample into two with average $Q^2 = 21$ (GeV/c^2)^2 and $Q^2 = 99$ (CeV/c^2)^2. Together with the FEMC sample it gives four subsamples covering average Q^2 from 21 to 400 (GeV/c^2)^2. In Fig.4, energy flow for jets in the rapidity scale is plotted for those four Q^2 regions. There is quite reasonable agreement in all these plots observed except slight shifts. Here rapidity was calculated from the direction of tagged electron, which is located in the rapidity region from -4.0 to -2.5, but it is not shown on

the plot. Many other distributions were compared with mode l predictions and none of them was found to be in clear disagreement.

5. THE F_2^γ ESTIMATIONS

Usually the hadronic structure function of the photon F_2^γ is extracted from the measurements by the unfolding procedure. This procedure reconstructs x_{true} from x_{visible} and converts x_{true} to the F_2^γ. Several problems have been discovered recently in this procedure. First of all, it comes out that this procedure is very much model-dependent. The final result depends on the model used in the unfolding, namely on the filial state topology which defines the correlation between x_{true} and x_{visible} and conversion factor between x_{true} and F_2^γ. Another uncertainty is in the choice which of the components or their combinations should be changed to get an agreement between data and model prediction. This point is essentially unclear in case of generators which do not allow an explicit separation of events of different types but internally have this separation. All these questions have to be answered to make unfolding procedure adequate to the problem under study.

In present study already from Fig.5 one can see that the structure function extracted from the data should be in agreement with the one used in TWOGAM (at least within the experimental error). It slightly simplifies the extraction of F_2^γ from the data. The only goal for such an extraction

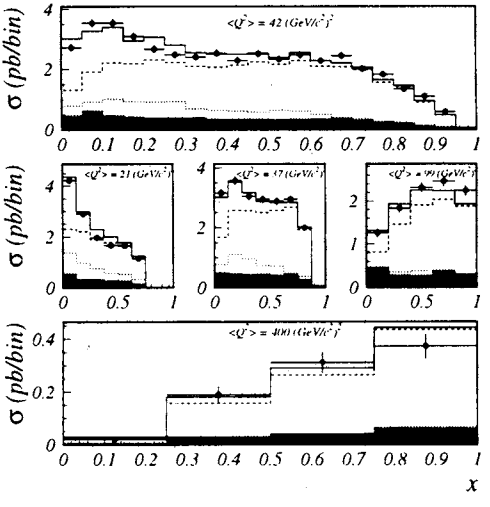

Fig. 5. Comparison between data and Monte Carlo predictions for x distributions in different Q^2 regions. Points are data, and the histograms show the Monte Carlo predictions. QPM+GVDM+RPC — solid line, GVDM+QPM — dashed line, GVDM — dotted line, hatched area is the background estimate

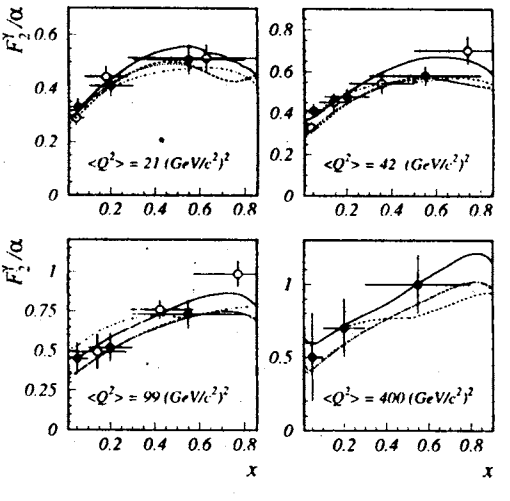

Fig. 6. The measurements of F_2^γ for the four Q^2 regions. Open circles show the unfolded values of F_2^γ black circles are F_2^γ estimates made by the simple algorithm. Solid lines are a TWOGAM predictions for the F_2^γ. Lines are the GS (dashed-dotted), GRV (dashed) and SaS (dotted) predictions for the F_2^γ

Table. Summary for the unfolding in three bins

Q^2, GeV^2/c^4	x range	F_2^γ/α
21	0.01-0.1	0.33 ± 0.01 ± 0.03
	0.1-0.3	0.41 ± 0.03 ± 0.02
	0.3-0.8	0.51 ± 0.05 ± 0.04
42	0.01-0.1	0.41± 0.01 ± 0.03
	0.1-0.3	0.48 ± 0.02 ± 0.02
	0.3-0.8	0.59 ± 0.03 ± 0.04
99	0.01-0.1	0.45 ± 0.06 ± 0.02
	0.1-0.3	0.52 ± 0.05 ± 0.03
	0.3-0.8	0.73 ± 0.05 ± 0.03
400	0.01-0.1	0.5 ± 0.3 ± 0.1
	0.1-0.3	0.7 ± 0.2 ± 0.2
	0.3-0.8	1.0 ± 0.1 ± 0.3

in this case is to show the accuracy of this agreement and indicate the regions of slight deviations if any.

Simple algorithm has been used in this study to estimate F_2^γ. The x_{true} distributions for each component have been subdivided into three bins and each bin content was varied in the wide region using scale factors α_k ($k = 1,3$) to get a better agreement for different visible distributions. For each α_k a set of visible distributions was fitted to model predictions, then χ^2 vs α_k dependents were used to determiner α_k corresponding to the χ^2_{min} together with statistically accepted range of α_k to estimate the error of α_k. The structure functions for each of the components in the model were used to transform $x_{\text{true}}\alpha_k$ distributions to the structure function. By varying selection criteria and applying artificial shifts of some variables in the data (E_{tag}, Q^2, W) the systematic error was determined by the same procedure. The results are shown in Fig.6 by black circles and in the Table.

Blobel's program [6] has been used to estimate F_2^γ well. The QPM events were used to perform unfolding. The VDM and the RPC events were treated as a background. To get prediction for the total F_2^γ the theoretical predictions for the VDM and RPC structure functions used in the TWOGAM have been added to unfolded point-like component of F_2^γ. The results are shown in Fig.6 by open circles.

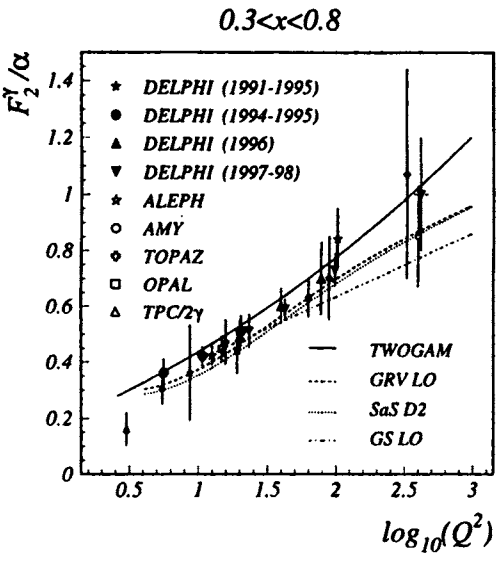

Fig. 7. The measurements of F_2^γ averaged in the x range $0.3 < x < 0.8$ as a function of Q^2. Some of the points measured by other collaborations are taken from the published plots, so slight shift may be present

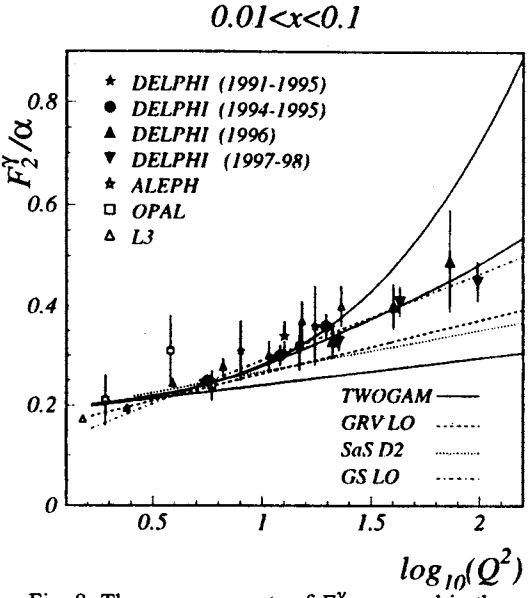

Fig. 8. The measurements of F_2^γ averaged in the x range $0.01 < x < 0.1$ as a function of Q^2. Some of the points measured by other collaborations are taken from the published plots, so slight shift may be present

The results of these two procedures are similar but in contrast with the unfolding procedure the algorithm used is much more transparent and well under control. The table shows the summary results for the structure function study.

The statistical and systematic errors are given separately in the right column. The predictions of some models are also plotted in Fig.6 (SaS [7], CRV [8], GS [5]). The models chosen here are the most popular in recent studies and those from possible sets which are closer to experimental points. Figure 7 shows the average F_2^γ for conventional range $0.3 < x < 0.8$ as a function of $\log(Q^2)$. Measurements of average F_2^γ as a function of $\log(Q^2)$ in the low region (from 0.01 to 0.1) are presented in Fig.8. The model predictions are also shown. Results obtained by other collaborations are shown on the same plots and most of them are in agreement with present measurements. The function $p_1 + p_2 \ln(Q^2)$ is used to fit DELPHI data from Figs. 7,8. The fit result for the high region is:

$$F_2^\gamma/\alpha = (0.9 \pm 0.05) + (0.14 \pm 0.02)\ln(Q^2).$$

For the low x region the result is:

$$F_2^\gamma/\alpha = (0.12 \pm 0.02) + (0.073 \pm 0.009)\ln(Q^2).$$

6. CONCLUSIONS

The data samples taken by the DELPHI experiment at LEP during 1996–1998 have been used to study the hadronic structure function of the photon. The hadronic final state is found to be best represented by a mixture of three components based on the Vector Meson Dominance model, QPM model and resolved photon component. The third component is essentially important in the low x region and makes possible to describe data much better, especially the event variables which are not strongly correlated with x_{true} and whose description cannot be improved by tuning the shape of the structure function.

The first check of the model including RPC given by the GS parameterization (set 2) has been done in our no-tag analysis [1] at LEP1, where a good agreement between data and the three component model was demonstrated. Later this model was tested for single tagged events in the region of very low Q^2 [9] and in the DIS study [10]. Thus it is demonstrated that the model describes data quite well in the wide Q^2-region. For the first time TWOGAM has been tuned to get a good agreement in the region of high Q^2. This tuning will not affect our previous study because suppression becomes significant in the region above $Q^2 = (\mathrm{GeV/c}^2)^2$.

The event sample has been used to estimate the hadronic photon structure function, F_2^γ. These measurements are found to be compatible with model expectations taken from different parameterizations of the parton distributions of the photon. At the same time these parameterizations implemented in the general parton generators PYTHIA or HERWIG give quite differed results both from the data and each other.

The main question which should be answered now is not a structure function shape but how to treat this shape in the Monte Carlo generators. Why do so similar theoretical predictions (SaS, GRV, GS, TWOGAM) give very different results after their implementations in the PYTHIA, HERWIG or TWOGAM is the question to answer first.

7. ACKNOWLEDGEMENTS

We are greatly indebted to our technical collaborators an to the funding agencies for their support in building and operating the DELPHI detector, and to the members of the CERN SL Division for the excellent performance of the LEP collider.

We thank Gerhard A. Shuler and Torbjorn Sjostrand for help and very useful discussions.

References

1. DELPHI Coll., Abreu P. et al. — Z. Phys., 1994, v.C62, p.3.
2. DELPHI Col., Aarnio P. et al. — Nucl. Instr. and Meth., 1991, v.A303, p.233.
3. Nova S., Olshevsky A., Todorov T. — DELPHI-90-35 (unpublished).
4. Sjustrand T. — Comp. Phys. Comm., 1994, v.82, p.74.
5. Gordon I. E., .Storrow J.K. — Z. Phys., 1992, v.C56, p.307.

6. Blobel V. — In: Proceedings of the CERN School of Computing, Aiguablava, Spain, 1984, CERN 85-09.
7. Schuler G.A., Sjostrand T. — CERN-TH/95-62.
8. Glück M., Reya E., Vogt A. — Phys.Rev., 1992, v.D46, p.1973.
9. DELPHI Coll., Abreu P. et al. — Phys.Lett., 1995, v.B342, p.402.
10. DELPHI Coll, Tyapkin I. — Proc. of the 28th International Conference on High Energy Physics, Warsaw, Polland, World Scientific Publishing Co. Pte. Ltd. 1996, p.729.

Received on January 13, 1999